ELSEVIER

NeuroImage

www.elsevier.com/locate/ynimg
NeuroImage 28 (2005) 869 – 880

Quantitative evaluation of three cortical surface flattening methods

Lili Ju,[a,1] Monica K. Hurdal,[b] Josh Stern,[c] Kelly Rehm,[d] Kirt Schaper,[c] and David Rottenberg[c,d,e,*]

[a]*Institute for Mathematics and its Applications, University of Minnesota, Minneapolis, MN 55455, USA*
[b]*Department of Mathematics, Florida State University, Tallahassee, FL 32306-4510, USA*
[c]*Department of Neurology, University of Minnesota, Minneapolis, MN 55455, USA*
[d]*Department of Radiology, University of Minnesota, Minneapolis, MN 55455, USA*
[e]*Neurology Service, Minneapolis VA Medical Center, Minneapolis, MN 55417, USA*

Received 4 August 2004; revised 15 February 2005; accepted 28 June 2005
Available online 19 August 2005

During the past decade, several computational approaches have been proposed for the task of mapping highly convoluted surfaces of the human brain to simpler geometric objects such as a sphere or a topological disc. We report the results of a quantitative comparison of FreeSurfer, CirclePack, and LSCM with respect to measurements of geometric distortion and computational speed. Our results indicate that FreeSurfer performs best with respect to a global measurement of metric distortion, whereas LSCM performs best with respect to angular distortion and best in all but one case with a local measurement of metric distortion. FreeSurfer provides more homogeneous distribution of metric distortion across the whole cortex than CirclePack and LSCM. LSCM is the most computationally efficient algorithm for generating spherical maps, while CirclePack is extremely fast for generating planar maps from patches.

Keywords: Cortical surface flattening; Angular distortion; Metric distortion

Introduction

Since the highly convoluted cerebral and cerebellar cortices are topologically equivalent to a two-dimensional sheet (topological sphere or disc), surface representations of the cortex should facilitate the visualization and analysis of functional activation data by preserving important geometrical and topological relationships. Moreover, surface representations which can be parameterized using two-dimensional coordinate systems (i.e., flat maps) may be useful for anatomically driven inter-subject registration (Van Essen et al., 1998).

Various methods have been proposed to inflate and/or flatten cortical brain surfaces: CARET (Drury et al., 1996), FreeSurfer (Fischl et al., 1999), the Laplace–Beltrami operator (Angenent et al., 1999), circle packing (via the CirclePack software) (Hurdal et al., 1999), harmonic energy minimization (Gu and Yau, 2002), and Least Squares Conformal Mapping (LSCM) (Ju et al., 2004). Although flattening a cortical surface necessarily introduces metric distortion due to the non-constant Gaussian curvature of the surface, it is possible to preserve local angular information ("conformality") (Ahfors, 1996). We call a mapping that keeps conformality of the surfaces a "conformal mapping". Pioneering work on numerical implementation of spherical conformal mapping was done by Brechbuhler et al. (1995) and Szekely et al. (1996) for the purpose of surface parameterization.

In order to quantify angular and metric distortion using conformal mapping techniques and non-conformal methods, we examined the performance of three published, freely available surface-mapping algorithms: FreeSurfer, CirclePack, and LSCM. All three methods can flatten user-defined patches and produce two-dimensional spherical surface maps of cortical hemispheres. CARET and FreeSurfer are similar in that both algorithms explicitly minimize metric distortion by solving a large-scale nonlinear optimization problem. The other four algorithms listed above produce discrete quasi-conformal maps. The Laplace–Beltrami operator, harmonic energy minimization, and LSCM are based on different but equivalent definitions of conformal mapping. They use both vertex connectivity and metric information, whereas tangency-based circle packing makes use of metric information from only the surface boundary, and otherwise depends only on the vertex connectivity of the surface mesh. All of the algorithms mentioned above work with the input surface meshes directly, and do not attempt to either reduce or subdivide the mesh.

Methods

Flattening techniques

Let $\mathcal{K}$ be a simply connected triangulated cortical surface $\left\{\{\mathbf{v}_i\}_{i=1}^n, \mathcal{T} = \{T_i = (\mathbf{v}_{i_1}, \mathbf{v}_{i_2}, \mathbf{v}_{i_3})\}_{i=1}^m\right\}$ where $\{\mathbf{v}_i\}_{i=1}^n$ is a set of n

* Corresponding author. Neurology Service, Minneapolis VA Medical Center, Minneapolis, MN 55417, USA.
E-mail address: dar@neurovia.umn.edu (D. Rottenberg).
[1] Current address: Department of Mathematics, University of South Carolina, Columbia, SC 29208, USA.
Available online on ScienceDirect (www.sciencedirect.com).

1053-8119/$ - see front matter © 2005 Elsevier Inc. All rights reserved.
doi:10.1016/j.neuroimage.2005.06.055

Table 1
Comparison of features of three flattening methods

Feature/Capability	FreeSurfer	CirclePack	LSCM
Flat map premise?	Metric	Conformal	Conformal
What is optimized directly?	Metric distortion	Finding a packing	Conformal energy
Geometrically converges?	No	Yes	Yes
Mesh information used?	Metric and combinatoric	Metric on boundary and combinatoric elsewhere	Metric and combinatoric
Finds global optimum?	No	Yes	Yes
Global optimum unique?	No	Up to Möbius	Up to Möbius
Spherical map	Yes	Yes	Yes
Planar map: unspecified shape	Yes	Yes	Yes
Planar map: specific shape	No	Yes (convex)	Yes (convex)

vertices with $n \geq 3$ and $\mathcal{T}$ is a set of m triangles consisting of triples of vertices. Assume that $\mathcal{K}$ is consistently oriented. Then each triangle of $\mathcal{T}$ has a uniquely defined normal.

Let $\mathcal{U}$ represent the flattening function. Assume that $\mathcal{U}$ is linear on each triangle T_i, implying that the flattening can be uniquely determined by the mapping of the vertices of $\mathcal{K}$. Let $T_i^{\mathcal{U}} = \mathcal{U}(T_i)$ denote the mapping triangle of T_i. Let $A(T_i)$ and $A\left(T_i^{\mathcal{U}}\right)$ denote the oriented area of triangle T_i on the cortical surface $\mathcal{K}$ and its flat map $\mathcal{U}(\mathcal{K})$, respectively. Let $d_{i,j}$ and $d_{i,j}^{\mathcal{U}}$ denote the geodesic distances between the vertex $\mathbf{v}_i$ and $\mathbf{v}_j$ on the cortical surface $\mathcal{K}$ and its flat map $\mathcal{U}(\mathcal{K})$, respectively. A modified *Dijkstra Algorithm* (Dijkstra, 1959) is employed to compute the geodesic distances on the polyhedral surface as suggested in Fischl et al. (1999). Although there are some more accurate algorithms (Kanai and Suzuki, 2001; Mitchell et al., 1987), they are either computationally infeasible for large meshes or else prohibitively difficult to implement.

A conformal map preserves angles and angle direction. In order to conformally map a discrete surface embedded in $\mathbb{R}^3$ to a surface of constant curvature such as the plane, $\mathbb{C}$ (if $\mathcal{K}$ is a topological disc), or a sphere, $\mathcal{S}^2$ (if $\mathcal{K}$ is a topological sphere), the mapping should preserve discrete angle *market share* at each vertex (Hurdal et al., 1999; Hurdal and Stephenson, 2004). The spherical conformal maps of $\mathcal{K}$ are not unique since the sphere $\mathcal{S}^2$ has a rich group of *automorphisms*, i.e., one-to-one conformal maps from $\mathcal{S}^2$ to itself. The automorphism group of $\mathcal{S}^2$, Aut $(\mathcal{S}^2)$ is the group of all Möbius transformations of $\mathcal{S}^2$, i.e.,

$$\mathrm{Aut}(\mathcal{S}^2) = \left\{ \psi | \psi : z \rightarrow \frac{az+b}{cz+d}, a,b,c,d \in \mathbb{C}, ad-bc \neq 0 \right\}.$$

Choosing three points, such as anatomical landmarks, is one way to specify the Möbius transformation.

Since conformal maps are synonymous with angle preservation, they make no attempt to minimize metric distortion. The flexibility in choosing a Möbius transformation enables us to choose such a transformation that minimizes metric distortion within the group of automorphisms. Therefore, for the purposes of comparing metric distortion between conformal maps and metric-based methods, we have added a final step to the conformal mapping algorithms. The spherical conformal map $\mathcal{U}$ is normalized by finding a Möbius transformation $\psi \in \mathrm{Aut}(\mathcal{S}^2)$ that minimizes the metric distortion among the automorphism group. This is a small-scale nonlinear optimization problem which can be quickly solved by *Powell's Method* (Powell, 1964).

FreeSurfer

FreeSurfer is a very popular software package for cortical surface inflation and flattening that explicitly minimizes the metric distortion of the flattened cortical surface. It inflates a surface by attempting to minimize the following mean-squared energy functional:

$$\mathbf{J}_d = \frac{1}{4n} \sum_{i=1}^{n} \sum_{j \in N(i)} \left(d_{i,j}^{\mathcal{U}} - d_{i,j} \right)^2$$

where $N(i)$ denotes the index set of vertices which are predefined neighbors of vertex i, and distances are approximations of geodesic distance computed by the same method cited above. Since it is not feasible to unfold a large cortical surface by simply minimizing the distance term, another functional related to oriented area is added:

$$\mathbf{J}_a = \frac{1}{2m} \sum_{i=1}^{m} P\left(A\left(T_i^{\mathcal{U}}\right)\right)\left(A\left(T_i^{\mathcal{U}}\right) - A(T_i)\right)^2$$

where $P\left(A\left(T_i^{\mathcal{U}}\right)\right) = 1$ if $A\left(T_i^{\mathcal{U}}\right) > 0$, otherwise $P\left(A\left(T_i^{\mathcal{U}}\right)\right) = 0$.

Then, the complete functional becomes

$$\mathbf{J} = \lambda_d \mathbf{J}_d + \lambda_a \mathbf{J}_a \tag{1}$$

where λ_a and λ_d define the relative importance of unfolding versus the minimization of metric distortion. Initially λ_a takes much larger values than λ_d and gradually decreases over time as the surface is successfully unfolded. A *Multi-scale Line Minimization* (Press et al., 1994) scheme is used to solve this nonlinear optimization problem (Eq. (1)). FreeSurfer is not guaranteed to find the global minimum of this function. Due to the fact that it uses a modified Dijkstra (graphbased) algorithm to compute distances between vertices, FreeSurfer's results may be affected by retriangulations of the surface mesh which do not change the 3D spatial position of the mesh, because the retriangulation would affect both the set of vertices available for distance computations and the estimated geodesic distances between them.

A spherical map is generated through projecting the inflated cortical surface onto the sphere by moving each vertex to the closest point on the sphere. The energy functional is again minimized to reduce the metric distortion and remove any folds introduced by the projection process.

Table 2
Mesh information of the cortical surfaces

Cortical surfaces	Cerebral cortex	Cerebellar hemisphere	
		MNI	UPENN
Vertices	28,340	191,724	146,922
Triangles	56,676	383,444	293,840

Table 3
Mesh information and percentage of hemispheral area of the cerebral lobar patches

Cerebral lobar patches		Vertices	Triangles	Boundary vertices	Percentage of hemispheral area
Frontal lobe	MNI	59,319	117,944	692	31.04
	UPENN	48,311	95,776	844	32.92
Occipital lobe	MNI	27,649	54,796	500	14.34
	UPENN	17,102	33,823	379	11.46
Parietal lobe	MNI	37,884	74,921	845	19.74
	UPENN	28,812	56,915	707	19.66
Temporal lobe	MNI	42,631	84,568	692	21.80
	UPENN	33,971	67,365	575	22.03

Table 4
CPU time and angular and metric distortion (I and II) of spherical maps of the MNI cerebellar cortex produced by FreeSurfer, CirclePack, and LSCM

Spherical map of cerebellar cortex		FreeSurfer	CirclePack	LSCM
CPU time (min)		35.3	53.73	0.9
Angular distortion (°)	Mean	15.25	15.03	1.91
	SD	14.55	15.86	2.56
Metric distortion I (%)	Mean	19.35	35.57	36.58
	SD	10.27	20.02	21.94
Metric distortion II (%)	Mean	14.34	14.98	10.71
	SD	6.33	8.19	5.38

CirclePack

CirclePack is a discrete conformal flattening method that preserves angular proportions locally. Its simplest implementation uses tangency circle packing which depends solely on the mesh vertex connectivity when there is no surface boundary. Thus, it does not take into account metric information about the relative edge lengths of the original cortical surface unless the surface has a boundary.

A tangency circle packing can be described as follows: a collection of circles $\mathbf{C}_{\mathcal{K}} = \{C(\mathbf{v}_i)\}_{i=1}^{n}$ in the plane, one circle for each vertex $\mathbf{v}_i$, has the property that $C(\mathbf{v}_i)$ and $C(\mathbf{v}_j)$ are tangent whenever $\mathbf{v}_i$ and $\mathbf{v}_j$ form an edge of $\mathcal{K}$. The *Circle Packing Theorem* states that given any triangulation of a topological disc, $\mathcal{K}$, and any assignment of positive numbers $r_1, r_2, \ldots, r_{n_b}$ to the boundary vertices $\mathbf{v}_1, \mathbf{v}_2, \ldots, \mathbf{v}_{n_b}$ of $\mathcal{K}$, there is a unique (up to a Euclidean isometry) tangency circle packing in the plane with boundary circle $C(\mathbf{v}_i)$ having radius r_i (Rodin and Sullivan, 1987). In general, $r_1, r_2, \ldots, r_{n_b}$ can be set to be proportional to the lengths of the corresponding boundary edges in $\mathcal{K}$ as we did in our numerical experiments. It is noted that if $\mathcal{K}$ consists only of equilateral triangles, then its circle packing will be conformal.

The packing pattern for Euclidean or Hyperbolic map (i.e., $\mathcal{K}$ is a topological disc) is found by an iterative method (Collins and Stephenson, 2003) and regarded as the resulting flat map $\mathcal{U}$. If $\mathcal{K}$ is a topological sphere, first an arbitrary vertex $\mathbf{v}^*$ chosen from $\{\mathbf{v}_i\}_{i=1}^{n}$ and all edges containing it are removed from the input triangulated mesh $\mathcal{K}$, clearly, the pruned mesh $\mathcal{K}'$ becomes a topological disc. Then, spherical maps are generated by stereographic projection of the circle radii from the Hyperbolic map of $\mathcal{K}'$ computed using CirclePack and mapping $\mathbf{v}^*$ to the *north pole*. The spherical map is finally normalized by finding a Möbius transformation that minimizes the metric distortion among the automorphism group.

In our experiments, we tested CirclePack on a general mesh featuring non-equilateral triangles. Although it would seem that CirclePack should be sensitive to the triangulation obtained from the MRI images, preliminary numerical experiments have shown that this is not the case. This could be attributed to the fact that a given triangulation encodes angular and curvature information from the surface and so the triangulation is not arbitrary. The CirclePack maps do not seem to change significantly if a triangulation is changed or decimated as long as the main curvature features are maintained.

LSCM

LSCM (least squares conformal mapping) was originally conceived as a planar conformal parameterization method based on a least-squares approximation of the *Cauchy–Riemann equation* (Levy et al., 2002). Suppose that $\mathcal{K}$ is a topological disc and consider a smooth map $\mathcal{U}: \mathcal{K} \to \mathbb{R}^2$. When restricting $\mathcal{U}$ on one of the triangles of $\mathcal{T}$, say T, the Cauchy–Riemann equation states that $\mathcal{U}$ is conformal on T if and only if $\frac{\partial \mathcal{U}}{\partial x} + i\frac{\partial \mathcal{U}}{\partial y} = 0$ holds true everywhere on $\mathcal{T}$. This conformal criterion generally cannot be strictly satisfied on the whole triangulated surface $\mathcal{K}$ embedded in $\mathbb{R}^3$. Violations of this condition are minimized in order to construct a quasi-conformal map in the least squares sense:

$$\min_{\mathcal{U}} C(\mathcal{K}) = \sum_{T \in \mathcal{T}} \int_T \left| \frac{\partial \mathcal{U}}{\partial x} + i\frac{\partial \mathcal{U}}{\partial y} \right|^2 dA = \sum_{T \in \mathcal{T}} \left| \frac{\partial \mathcal{U}}{\partial x} + i\frac{\partial \mathcal{U}}{\partial y} \right|^2 A(T).$$

Suppose that $\mathbf{u}_i = \mathcal{U}(\mathbf{v}_i)$ for $i = 1, \ldots, n$, then $C(\mathcal{K})$ can be written in *quadratic form* such as:

$$\min_{\mathcal{U}} C(\mathcal{K}) = \mathbf{u}^* M^* M \mathbf{u} \tag{2}$$

where $\mathbf{u} = (\mathbf{u}_1, \ldots, \mathbf{u}_n)$ and M is an $m \times n$ complex matrix and * represents matrix conjugate transpose. To make the minimization problem (Eq. (2)) have a unique and non-trivial solution, some of the $\mathbf{u}_i's$ must be pre-defined. Let us re-arrange the vector $\mathbf{u}$ such that $\mathbf{u} = (\mathbf{u}_f, \mathbf{u}_p)$ where $\mathbf{u}_f$ consists of $n-q$ free coordinates and $\mathbf{u}_p$ consists of q pinned coordinates. Then, Eq. (2) can be rewritten as $C\mathcal{K} = ||M_f \mathbf{u}_f + M_p \mathbf{u}_p||^2$ where $M = (M_f, M_p)$ such that M_f is a $m \times (n-q)$ matrix and M_f, is a $m \times q$ matrix.

A minimization problem (Eq. (2)) of least squares type can be efficiently solved using *Conjugate Gradient Method* (Press et al.,

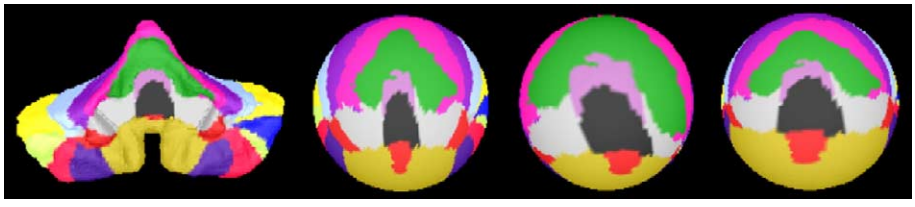

Fig. 1. From left to right: the MNI cerebellar cortex and spherical maps produced by FreeSurfer, CirclePack, and LSCM, respectively.

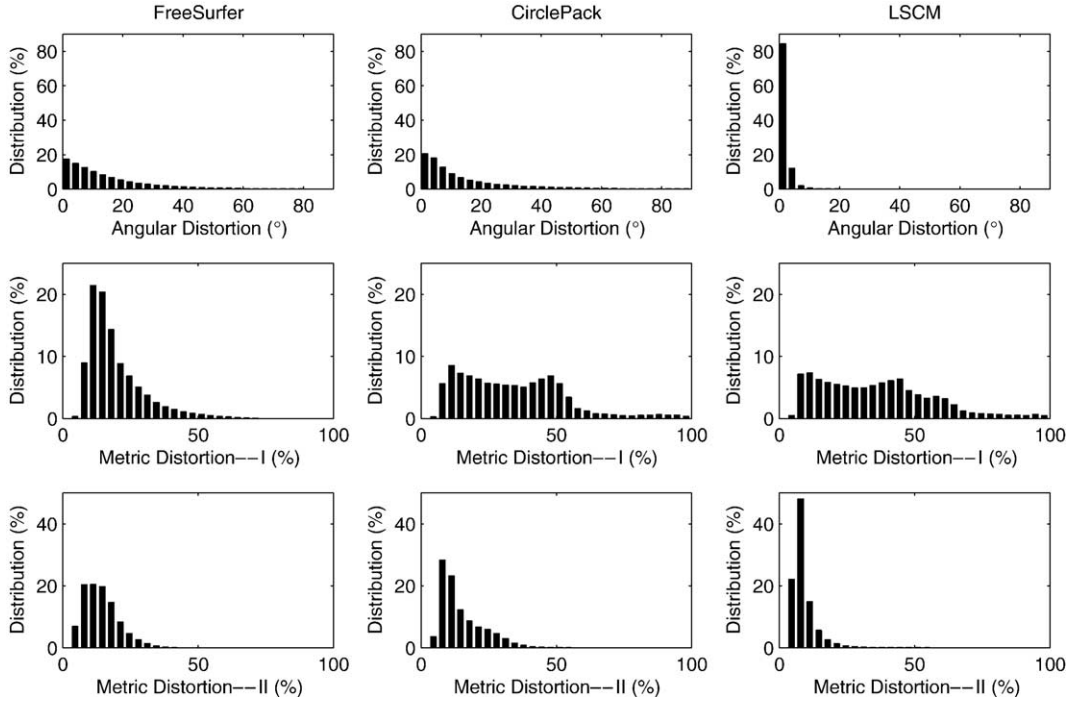

Fig. 2. Frequency histograms illustrating the angular and metric distortion (I and II) of spherical maps of the MNI cerebellar cortex generated by FreeSurfer (left), CirclePack (middle), and LSCM (right).

1994) and it has a unique solution when $q \geq 2$. In order to obtain the planar map with the least conformal distortion, q should be set to 2 (Levy et al., 2002). In our experiments, we set $q = 2$ and the two vertices maximizing the length of the shortest path between them were chosen to be pinned. Once again, if $\mathcal{K}$ is a topological sphere, the spherical map is obtained by stereographic projection using the same trick as CirclePack and normalized by finding a Möbius transformation that minimizes the metric distortion among the automorphism group.

When the size of the surface is very large and that of the boundary is relatively quite small, numerical conformal maps contain metric distortion that is often much greater in regions close the surface boundary than that of interior regions. The *Adaptive Weighted LSCM* approach was developed to solve this problem:

$$\min_{\mathcal{U}} C(\mathcal{K}) = \sum_{T \in \mathcal{T}} \alpha_T \left| \frac{\partial \mathcal{U}}{\partial x} + i \frac{\partial \mathcal{U}}{\partial y} \right|^2 A(T) \tag{3}$$

where $\alpha_T > 0$ is the weight for the triangle T. The weights are adaptively adjusted to penalize the unequal distribution of the areal distortion among the mesh triangles until some stopping criterion is satisfied. In our experiments, the following simple algorithm was used:

Algorithm

1. Initialize $\alpha_T = 1$ for all $T \in \mathcal{T}$ and set $k = 1$.
2. Solve the minimization problem (Eq. (3)) to obtain the current mapping $\mathcal{U}$.
3. Compute the areal distortion on each triangle $\{AD_T\}_{T \in \mathcal{T}}$ of the flat map $\mathcal{U}(\mathcal{K})$ after normalization. Then, calculate the corresponding standard deviation ST_k over all triangles.
4. If $ST_k > ST_{k-1}$ or $k \geq 8$, then stop; otherwise, set $\alpha_T = \alpha_T \left(1 + \frac{AD_T}{1+k^2}\right)$ for each T $\in \mathcal{T}$.
5. Normalize the weights $\{\alpha_T\}_{T \in \mathcal{T}}$ by their average and set $k = k + 1$, then go to step 1.

Maps produced using the adaptive LSCM have larger conformal distortion but reduced metric distortion compared to non-adaptive LSCM. Note that Adapative Weighted LSCM was only used in flattening cortical patches and not for generating spherical maps in our experiments.

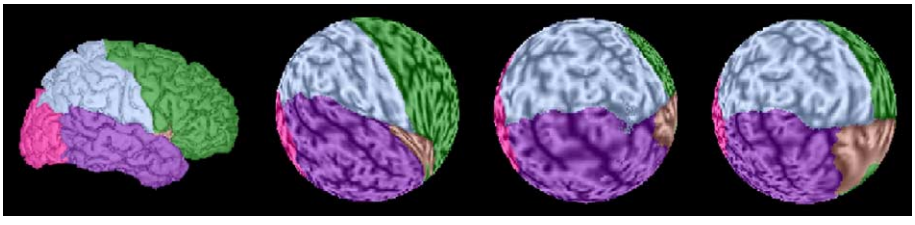

Fig. 3. From left to right: the MNI left cerebral hemisphere cortex (in radiological orientation) and spherical maps produced by FreeSurfer, CirclePack, and LSCM, respectively.

Table 5
CPU time and angular and metric distortion (I and II) of spherical maps of left cerebral hemisphere cortices produced by FreeSurfer, CirclePack, and LSCM

Spherical map of cerebral hemisphere			FreeSurfer	CirclePack	LSCM
MNI	CPU time (min)		630.5	2489.9	9.8
	Angular distortion (°)	Mean	18.75	16.55	4.63
		SD	15.83	15.18	4.57
	Metric distortion I (%)	Mean	26.06	37.86	33.70
		SD	12.37	22.48	20.10
	Metric distortion II (%)	Mean	18.88	20.84	11.79
		SD	7.49	13.84	7.06
UPENN	CPU time (min)		384.3	1265.6	19.2
	Angular distortion (°)	Mean	18.76	16.33	7.21
		SD	16.01	14.95	11.01
	Metric distortion I (%)	Mean	21.57	39.81	34.33
		SD	10.02	24.36	24.39
	Metric distortion II (%)	Mean	16.16	18.95	14.94
		SD	7.61	13.88	11.85

Comparison of features/capabilities

Features and capabilities of the above three flattening methods are summarized in Table 1. We comment on these distinctions as follows.

Flattening premise?—FreeSurfer is based on reducing metric distortion; LSCM and CirclePack are based on producing quasi-conformal maps that attempt to minimize or reduce conformal distortion.

What is optimized directly?—As described above, FreeSurfer iteratively reduces an approximate measure of metric distortion on local neighborhoods; CirclePack finds a packing (by iteratively minimizing the departure from local packing constraints around each mesh vertex) and implicitly assumes that the departure from conformality caused by the use of non-equilateral triangles is acceptable; LSCM directly minimizes a cost measure of departure from discrete conformality.

Geometrically converges?—Does the chosen cost function of each algorithm and the resulting flat map theoretically converge as the mesh granularity shrinks or is refined?

Mesh information used?—FreeSurfer and LSCM use both metric and connectivity information from the mesh, while the CirclePack implementation only employs metric information on the boundary and elsewhere only uses connectivity information.

Finds global optimum (of cost function)?—Because it depends on an iterative nonlinear optimization, FreeSurfer is not guaranteed to find a global minimum of its cost function and, in general, cannot know how far the local minimum that it does find is from the global maximum of the cost function; an algorithm that always converges to a circle packing is described by Collins and Stephenson; LSCM is a least squares problem which produces a linear system and can be efficiently solved by conjugate gradient method, so global convergence is guaranteed.

Is global optimum unique?—It is possible for the global optimum of FreeSurfer's cost function to be achieved by two or more significantly different mapping layouts; a circle packing is unique, and the linear equations generated by LSCM have a single basin of attraction. However, a conformal map is unique up to Möbius transformations so the final step of both LSCM and CirclePack depends on choosing an appropriate Möbius transformation. In order to compare the three methods, an optimized Möbius transformation that minimizes a metric distortion criterion is used, and it is theoretically possible for the global minimum value of this optimization to be achieved by two or more different Möbius transformations.

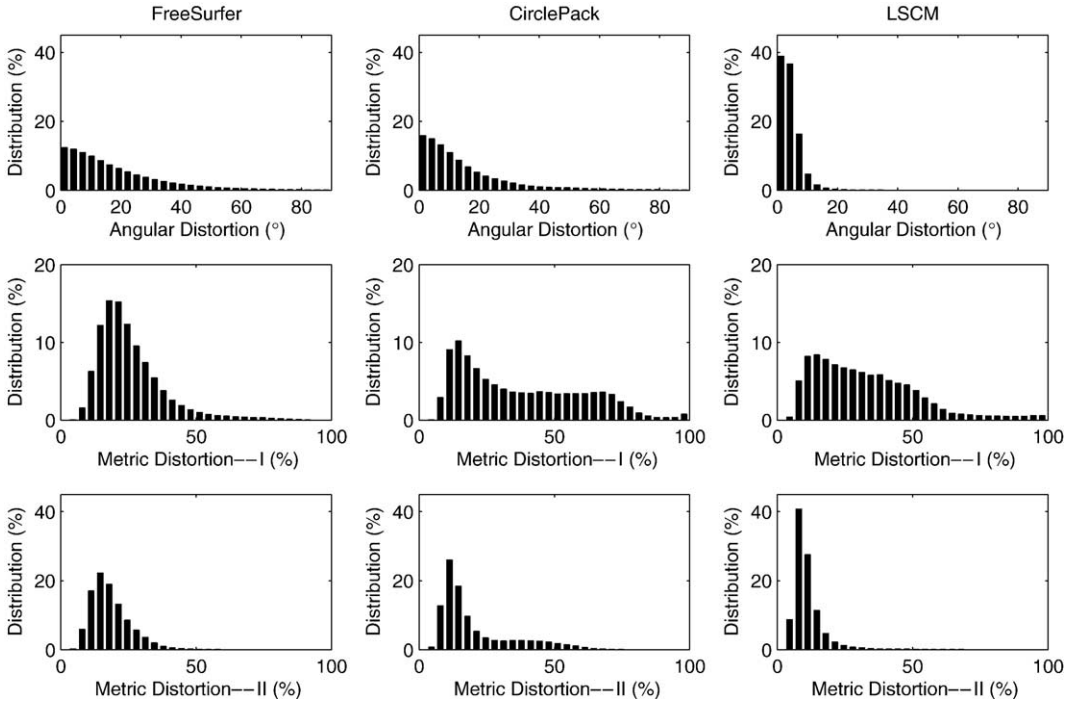

Fig. 4. Frequency histograms illustrating the angular and metric distortion (I and II) of spherical maps of the MNI left hemispheral cortex generated by FreeSurfer, (left), CirclePack (middle), and LSCM (right).

Spherical map—All of the methods can be used to map a mesh that is a topological sphere to a geometric sphere with the particular mapping determined by their respective criteria.

Planar map—All of the algorithms can map a mesh that is a topological disc to a planar region; however, the FreeSurfer software does not implement a method for mapping to a specific shape. Numerically, CirclePack and LSCM can map the mesh into any specific planar region, but theoretically the injectivity only can be guaranteed when the region is convex.

Measurements of distortion

We applied each algorithm to a number of cortical brain surface meshes and evaluated performance with respect to three different quantitative measures of geometric distortion defined below.

Angular distortion

Angular distortion is defined to reflect the difference between corresponding angles of the cortical surface $\mathcal{K}$ and its flat map $\mathcal{U}(\mathcal{K})$:

$$\mathcal{F}_{\text{ang}}(\mathcal{U}(\mathcal{K})) = \frac{1}{3\text{m}} \sum_{T_{ijk} \in \text{Face}(\mathcal{K})} \left(|\theta^{\mathcal{U}}_{ijk} - \theta_{ijk}| + |\theta^{\mathcal{U}}_{jki} - \theta_{jki}| + |\theta^{\mathcal{U}}_{kij} - \theta_{kij}| \right) \tag{4}$$

where T_{ijk} denotes the triangle formed by the vertices $\mathbf{v}_i$, $\mathbf{v}_j$, $\mathbf{v}_k$, θ_{ijk} denotes the angle $\angle \mathbf{v}_i\mathbf{v}_j\mathbf{v}_k$ on $\mathcal{K}$; and $\theta^{\mathcal{U}}_{ijk}$ denotes the angle $\angle \mathcal{U}(\mathbf{v}_i)\mathcal{U}(\mathbf{v}_j)\mathcal{U}(\mathbf{v}_k)$ on $\mathcal{U}(\mathcal{K})$. All interior angles on the cortical surface are normalized using the so-called market share of angles at vertices; in other words, the numbers used for each angle are proportional to the fraction of that angle in the sum of the angles around the vertex (this sum is always 2π radians on a flat mesh). The angular distortion of a discrete conformal map should theoretically go to zero as the granularity of the discrete mesh goes to zero and the mesh approximates a smooth surface.

Metric distortion

For each vertex, we label each of its nearest neighbors as a 1-neighbor, then we label each neighbor of a 1-neighbor that is not already labeled as a 2-neighbor. Repeating this process, we define k-neighbors for each vertex.

The first measure of *metric distortion* reflecting the global information (metric distortion I) is defined as follows:

$$\mathcal{F}_{\text{met-I}}(\mathcal{U}(\mathcal{K})) = \min_{s \in \mathbb{R}^+} \frac{1}{n} \sum_{i=1}^{n} \left(\frac{1}{\tilde{N}} \sum_{j \in N(i)} \frac{|s \cdot d^{\mathcal{U}}_{i,j} - d_{i,j}|}{d_{i,j}} \right) \tag{5}$$

where $N(i)$ is the pre-determined index set of neighbor vertices of the vertex $\mathbf{v}_i$ using the above definition of neighbors and $\tilde{N}$ = Card($N(i)$) [the cardinality of $N(i)$]. This metric measure is similar to the ones chosen in Fishcl et al. (1999) and Schwartz and Merker (1986) but with some obvious differences. Here, $s > 0$ is a scaling parameter used with the minimization process to avoid the influence of similarity transformations (in other words, the flat-mapping algorithm is not penalized for making the resulting flattened meshes have coordinates with a different absolute size scale than the original mesh). It is easy to see that $\mathcal{F}_{\text{met-I}}$ is the mean value of metric distortion of all vertices which is given by $\frac{1}{\tilde{N}} \sum_{j \in N(i)} |s \cdot d^{\mathcal{U}}_{i,j} - d_{i,j}| / d_{i,j}$ for any vertex $\mathbf{v}_i$.

Since it would be computationally prohibitive on large meshes to compute the value of our measure for all vertices using all choices of k, we performed a restricted subset of this measure. Specially, we set $N(i)$ to be the index set of all k-neighbors of $\mathbf{v}_i$ for $k \leq K$ for some $K > 0$. Then, $\{\mathbf{v}_j\}_{j \in i \cup N(i)}$ in fact forms a sub-mesh/subregion around $\mathbf{v}_i$ of the cortical surface. The larger K is (i.e., the more mutual metric information is used), the more

Table 6
Percentage of spherical area and angular and metric distortion (I and II) of spherical maps of left cerebral hemisphere cortices produced by FreeSurfer, CirclePack, and LSCM on lobar patches

Spherical map of cerebral hemisphere					
Cerebral lobe			FreeSurfer	CirclePack	LSCM
MNI	Frontal lobe	Percentage of spherical area	30.54	24.72	23.57
		Angular distortion (°)	15.88	23.72	4.37
		Metric distortion I (%)	22.76	58.73	32.90
		Metric distortion II (%)	16.35	33.02	10.53
	Occipital lobe	Percentage of spherical area	11.12	11.72	5.76
		Angular distortion (°)	18.69	11.96	4.47
		Metric distortion I (%)	25.61	25.22	40.78
		Metric distortion II (%)	18.71	13.81	11.84
	Parietal lobe	Percentage of spherical area	20.06	21.08	23.03
		Angular distortion (°)	18.75	12.81	4.19
		Metric distortion I (%)	24.73	22.84	22.18
		Metric distortion II (%)	19.93	14.14	9.65
	Temporal lobe	Percentage of spherical area	22.75	29.53	24.16
		Angular distortion (°)	19.07	13.26	4.70
		Metric distortion I (%)	27.98	29.40	33.21
		Metric distortion II (%)	19.55	15.63	13.14
UPENN	Frontal lobe	Percentage of spherical area	33.73	48.37	33.33
		Angular distortion (°)	17.63	17.93	7.56
		Metric distortion I (%)	18.67	42.91	31.50
		Metric distortion II (%)	15.13	20.71	14.00
	Occipital lobe	Percentage of spherical area	9.09	4.38	4.20
		Angular distortion (°)	16.87	14.60	5.75
		Metric distortion I (%)	20.39	38.67	45.63
		Metric distortion II (%)	15.54	14.94	13.15
	Parietal lobe	Percentage of spherical area	21.53	16.79	18.75
		Angular distortion (°)	17.27	14.73	5.52
		Metric distortion I (%)	18.74	30.80	28.12
		Metric distortion II (%)	14.84	17.53	14.57
	Temporal lobe	Percentage of spherical area	23.12	18.28	23.93
		Angular distortion (°)	18.48	13.96	5.83
		Metric distortion I (%)	20.64	34.47	31.41
		Metric distortion II (%)	16.09	14.99	12.91

the measure of metric distortion is reasonable and accurate. In our numerical experiments, K was set to be 15 (representing roughly circular patches of brain surface with a geodesic diameter of roughly 30 mm in our experiments), and consequently, $\tilde{N}$ becomes quite a large number. In order to efficiently calculate $\mathcal{F}_{\text{met-I}}$, we approximate some computations: we randomly sample 4 vertices from $N(i)$ at each level of neighbors and use this set of vertices as the new neighborhood $N(i)$ of $\mathbf{v}_i$ for the calculation of $\mathcal{F}_{\text{met-I}}$.

A second measure of *metric distortion*, reflecting local metric proportionality (metric distortion II) is measured as follows:

$$\mathcal{F}_{\text{met-II}}(\mathcal{U}(\mathcal{K})) = \frac{1}{n}\sum_{i=1}^{n}\left(\frac{1}{\tilde{N}}\min_{s_i\in\mathbb{R}^+}\sum_{j\in N(i)}\frac{|s_i\cdot d^{\mathcal{U}}_{i,j} - d_{i,j}|}{d_{i,j}}\right) \tag{6}$$

Here, we move the minimization process inside the first summation, i.e., the minimization process is done independently on its sub-mesh $N(i)$ for each vertex $\mathbf{v}_i$. There are n minimization processes in Eq. (6) but the complexity of each of them is much smaller than the one done in Eq. (5). The same neighborhood $N(i)$ defined above was used again for the computation of $\mathcal{F}_{\text{met-II}}$.

It is easy to see that $\mathcal{F}_{\text{met-I}}$ and $\mathcal{F}_{\text{met-II}}$ will be the same if $s_i = s$ for $i = 1,\ldots, n$, which means that the subregion formed by $\{\mathbf{v}_j\}_{j\in i\cup N(i)}$ associated with each vertex $\mathbf{v}_i$ is uniformly scaled in the flat map. We note that the $\mathcal{F}_{\text{met-II}}$ of a discrete conformal map should theoretically go to zero as the granularity of the discrete mesh goes to zero and mesh neighborhoods of every finite size approximate a smooth surface.

Cortical surfaces

Cortical surfaces of an isolated cerebellum and two left cerebral hemispheres were extracted from high-resolution T1-weighted MRI brain volumes obtained from the Montreal Neurological Institute (MNI) (Holmes and Hoge, 1996) and the University of Pennsylvania (UPENN). Triangular surface meshes (topological spheres) of the cortices were produced by an in-house region-growing algorithm (SurfMan) based on *Marching Cubes* (Lorensen and Cline, 1987), smoothed using a Gaussian kernel, and checked for topological correctness. In addition, frontal, occipital, parietal, and temporal lobar *patches* (topological discs) were *cut out* from both the MNI and PENN hemisphere surfaces using SnipMan, an in-house program that extracts a topological disc from a cortical surface. Descriptions of the cortical and lobar-patch meshes are presented in Tables 2 and 3. Cortical surfaces

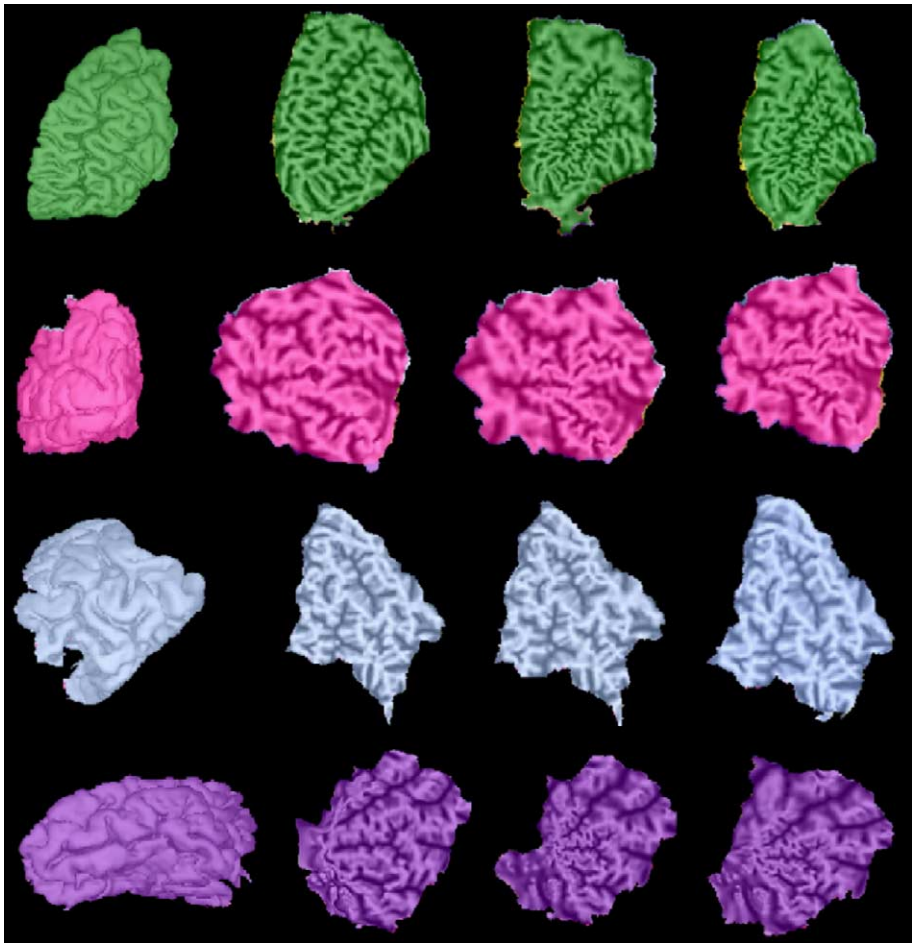

Fig. 5. From left to right: lobar patches cut from the MNI left hemisphere (in radiological orientation) and their planar maps generated by FreeSurfer, CirclePack, and LSCM, respectively. From top to bottom (row): frontal, occipital, parietal, and temporal patches.

Table 7
CPU time and angular and metric distortion (I and II) of planar maps of the frontal lobar patches produced by FreeSurfer, CirclePack, and LSCM

Planar map of frontal lobar patch			FreeSurfer	CirclePack	LSCM
MNI	CPU time (min)		276.50	2.10	56.80
	Angular distortion (°)	Mean	11.37	11.40	4.85
		SD	10.54	10.70	6.49
	Metric distortion I (%)	Mean	14.25	30.19	26.00
		SD	8.13	16.37	15.56
	Metric distortion II (%)	Mean	11.16	13.09	10.57
		SD	4.75	5.78	4.72
UPENN	CPU time (min)		279.40	1.25	61.40
	Angular distortion (°)	Mean	15.11	12.11	5.67
		SD	15.14	11.02	8.70
	Metric distortion I (%)	Mean	17.54	28.25	24.62
		SD	11.12	16.29	16.37
	Metric distortion II (%)	Mean	14.15	14.89	13.31
		SD	7.70	9.85	9.16

and lobar patches were then flattened using FreeSurfer, CirclePack, and LSCM.

Results and discussions

All three methods were run on a PC Linux workstation (1.67 GHz AMD Athlon XP CPU, 1.0 GB main memory) at the University of Minnesota. The default settings of the software were used. For the metric distortion computations, the sub-mesh associated with each vertex in the original mesh consisted of approximately 900 vertices with $K = 15$.

Cerebellar cortex

The parcellated surface of the MNI cerebellum and the spherical maps generated by FreeSurfer, CirclePack, and LSCM are illustrated in Fig. 1. Cortical regions defined by lobes and fissures were colored for identification purposes according to the criteria set by Schmahmann and his colleagues (Schmahmann et al., 2000). CPU time and measurements of angular and metric distortion (I and II) are reported in Table 4; corresponding frequency histograms are presented in Fig. 2. The least angular distortion (1.91°) and the least metric distortion II (10.71%) were produced by LSCM while the least metric distortion I (19.35%) was produced by FreeSurfer. CirclePack performed almost as same as LSCM on the metric distortion I and as FreeSurfer on the angular distortion. From Fig. 1, we could see that the Lobe III (green) seems much enlarged by CirclePack relative to other two methods and so does the Lobe IX (dark yellow) by LSCM. From Table 4, it also shows that LSCM ran much faster than FreeSurfer and CirclePack as expected.

Table 8
CPU time and angular and metric distortion (I and II) of planar maps of the occipital lobar patches produced by FreeSurfer, CirclePack, and LSCM

Planar map of occipital lobar patch			FreeSurfer	CirclePack	LSCM
MNI	CPU time (min)		157.50	0.35	14.30
	Angular distortion (°)	Mean	11.79	11.33	5.56
		SD	10.91	9.76	6.93
	Metric distortion I (%)	Mean	14.06	25.75	22.51
		SD	6.78	12.94	11.63
	Metric distortion II (%)	Mean	11.64	13.52	10.59
		SD	4.70	4.72	4.87
UPENN	CPU time (min)		247.40	0.30	7.80
	Angular distortion (°)	Mean	14.09	10.79	3.94
		SD	14.65	10.53	7.44
	Metric distortion I (%)	Mean	17.14	30.18	26.69
		SD	11.50	17.94	18.20
	Metric distortion II (%)	Mean	13.51	14.29	12.61
		SD	8.19	11.72	14.39

Table 9
CPU time and angular and metric distortion (I and II) of planar maps of the parietal lobar patches produced by FreeSurfer, CirclePack, and LSCM

Planar map of parietal lobar patch			FreeSurfer	CirclePack	LSCM
MNI	CPU time (min)		173.50	0.82	40.90
	Angular distortion (°)	Mean	7.30	11.50	4.05
		SD	7.05	9.72	6.69
	Metric distortion I (%)	Mean	8.93	18.21	14.64
		SD	3.30	8.28	9.48
	Metric distortion II (%)	Mean	7.70	12.27	8.51
		SD	2.59	3.46	3.39
UPENN	CPU time (min)		132.40	0.36	55.50
	Angular distortion (°)	Mean	13.37	11.06	4.54
		SD	13.58	10.29	5.73
	Metric distortion I (%)	Mean	15.07	23.65	26.93
		SD	9.83	14.79	17.99
	Metric distortion II (%)	Mean	12.30	14.17	13.89
		SD	7.04	8.13	10.19

Cerebral hemispheres

The parcellated surface of the MNI left cerebral hemisphere and the spherical maps generated by FreeSurfer, CirclePack, and LSCM are illustrated in Fig. 3. CPU time and measurements of angular and metric distortion (I and II) for spherical maps of both the MNI and UPENN cerebral hemispheres are reported in Table 5; corresponding frequency histograms for the MNI hemisphere are presented in Fig. 4. The least angular distortion (4.63° for MNI data and 7.21° for UPENN data) and metric distortion II (11.79% for MNI data and 14.94% for UPENN

Table 10
CPU time and angular and metric distortion (I and II) of planar maps of the temporal lobar patches produced by FreeSurfer, CirclePack, and LSCM

Planar map of temporal lobar patch			FreeSurfer	CirclePack	LSCM
MNI	CPU time (min)		282.50	1.36	18.70
	Angular distortion (°)	Mean	17.37	11.26	5.56
		SD	16.15	9.71	6.61
	Metric distortion I (%)	Mean	20.92	33.81	33.28
		SD	13.35	18.78	20.12
	Metric distortion II (%)	Mean	15.74	14.93	13.45
		SD	9.29	9.64	8.82
UPENN	CPU time (min)		229.40	1.10	61.10
	Angular distortion (°)	Mean	22.61	11.39	5.42
		SD	20.01	10.27	8.08
	Metric distortion I (%)	Mean	23.77	37.45	34.20
		SD	15.87	20.03	22.83
	Metric distortion II (%)	Mean	19.31	14.52	12.39
		SD	11.73	9.27	10.79

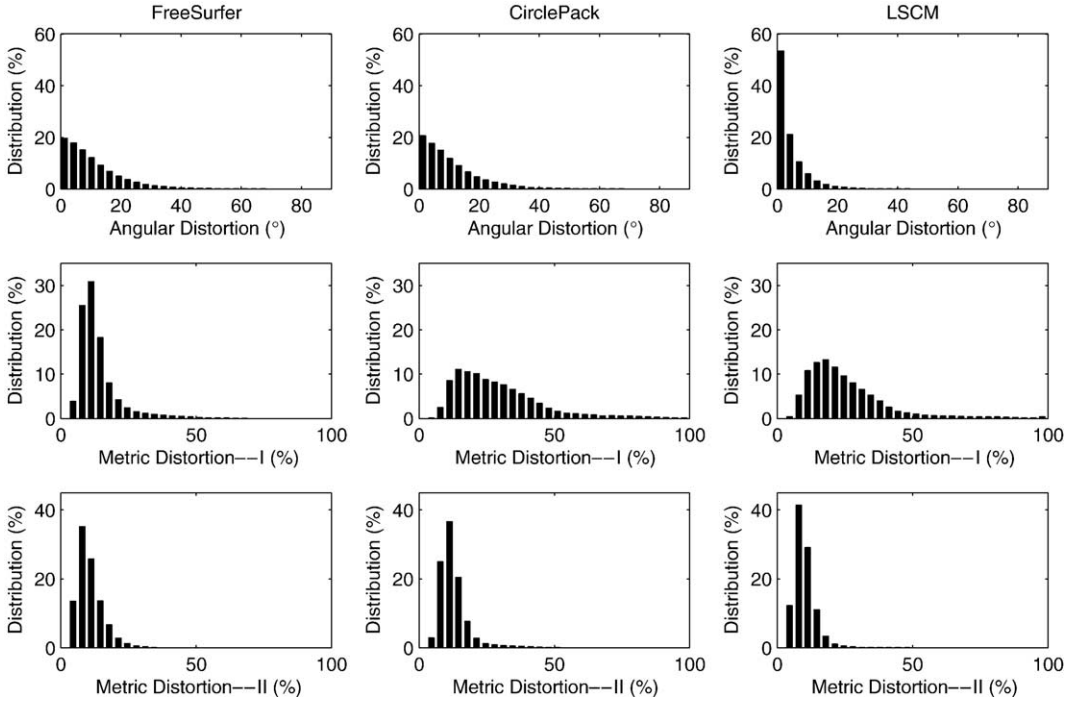

Fig. 6. Frequency histograms illustrating the angular and metric distortion (I and II) of planar maps of the MNI frontal lobar patch generated by FreeSurfer (left), CirclePack (middle), and LSCM (right).

data) were again produced by LSCM while the least metric distortion I (26.06% for MNI data and 21.57% for UPENN data) was again produced by FreeSurfer. CirclePack did not perform well in preserving angular information and also did worse than LSCM on the metric distortion I. Again, LSCM ran more than 20 times faster than FreeSurfer for both cerebral hemispheres.

In order to show how the distortion is spatially distributed across the cerebral hemisphere, we also report the results of corresponding percentage of spherical area, angular and metric

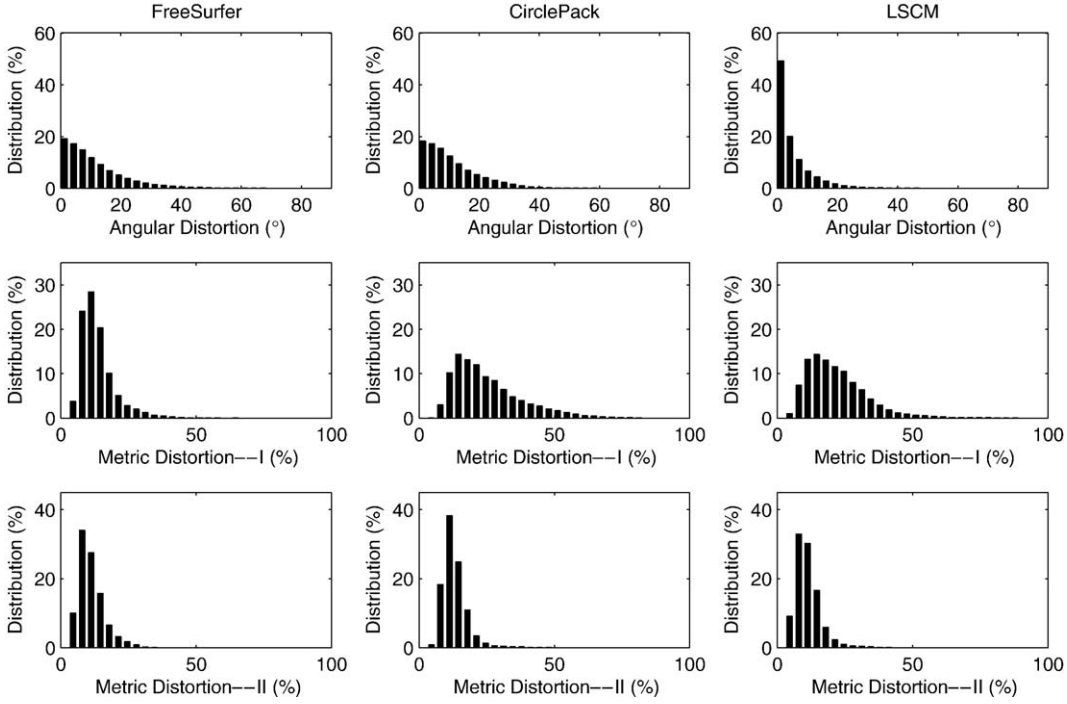

Fig. 7. Frequency histograms illustrating the angular and metric distortion (I and II) of planar maps of the MNI occipital lobar patch generated by FreeSurfer (left), CirclePack (middle), and LSCM (right).

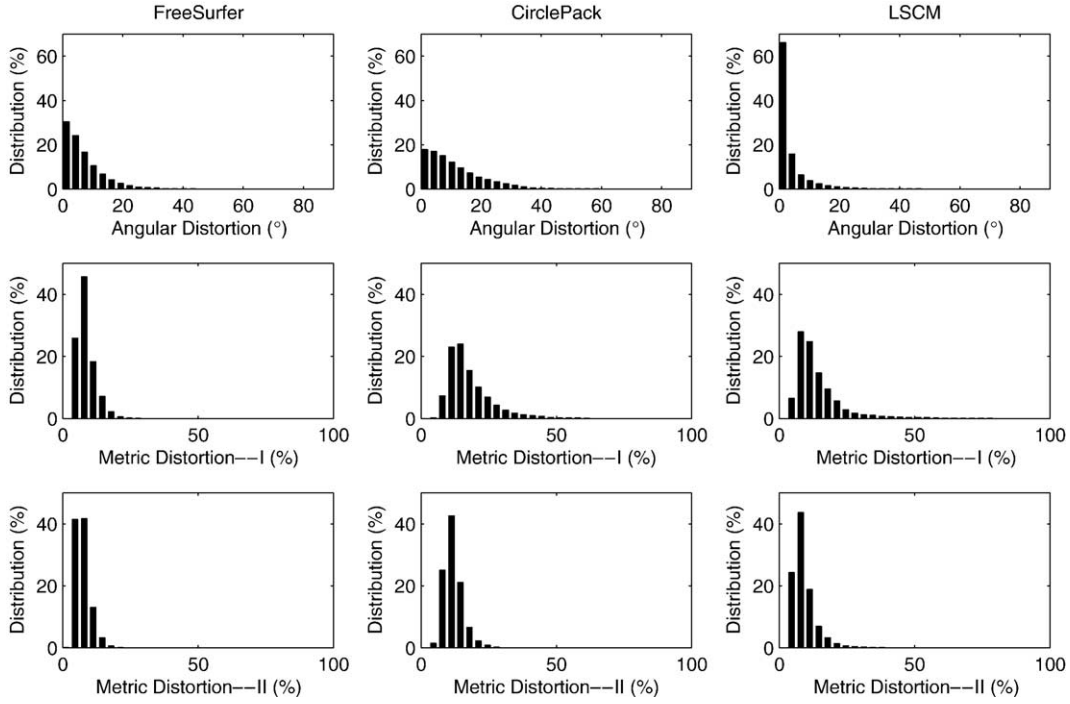

Fig. 8. Frequency histograms illustrating the angular and metric distortion (I and II) of planar maps of the MNI parietal lobar patch generated by FreeSurfer (left), CirclePack (middle), and LSCM.

distortion (I and II) of spherical maps of the left cerebral hemispheres on all lobar patches—frontal (green), occipital (pink), parietal (light blue), and temporal (purple) in Table 6. These data show that FreeSurfer exhibits more homogeneous distribution of metric distortion I across the whole cortex than CirclePack and LSCM for both the MNI and UPENN left cerebral hemispheres. FreeSurfer and LSCM both did better than CirclePack in uniformly distributing the angular distortion and metric distortion II. The temporal lobe of MNI data (percentage of area: 21.80% vs. 29.53%) and frontal lobe of UPENN data (percentage of area: 32.92% vs. 48.37%) are expanded by CirclePack relative to their original sizes; the occipital lobe

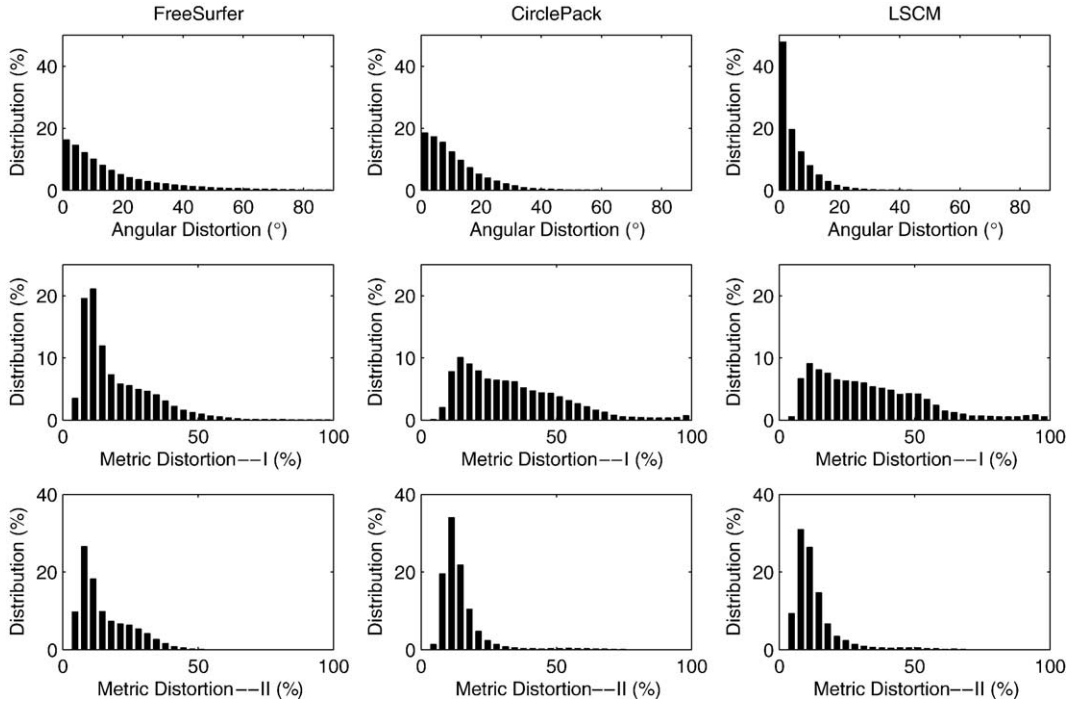

Fig. 9. Frequency histograms illustrating the angular and metric distortion (I and II) of planar maps of the MNI temporal lobar patch generated by FreeSurfer (left), CirclePack (middle), and LSCM (right).

(percentage of area: 14.34% vs. 5.76% for MNI data and 11.46% vs. 4.20%) for UPENN data is contracted by LSCM for both MNI and UPENN data sets.

Lobar patches

Lobar patches (frontal, occipital, parietal, and temporal lobes, respectively) cut from the MNI left hemisphere and their planar maps generated by FreeSurfer, CirclePack, and LSCM are illustrated in Fig. 5. CPU time and measurements of angular and metric distortion (I and II) for both the MNI and UPENN patches are reported in Tables 7–10; corresponding frequency histograms for the MNI lobar patches are presented in Figs. 6–9. In each case, the least angular distortion (4.85°, 5.56°, 4.05°, 5.56° for MNI lobar patches, respectively, and 5.67°, 3.94°, 4.54°, 5.42° for UPENN lobar patches, respectively) was produced by LSCM whereas the least metric distortion I (14.25%, 14.06%, 8.93%, 20.29% for MNI lobar patches, respectively, and 15.11%, 17.14%, 15.07%, 23.77% for UPENN lobar patches, respectively) was produced by FreeSurfer, but all three methods performed similarly with regards to metric distortion II. LSCM performed slightly better than CirclePack on metric distortion I. LSCM still ran faster than FreeSurfer even though the adaptive weighted approach was used. CirclePack's computations were extremely fast for all patches.

From the inspection of Fig. 5 (especially the sizes of sulci), it is easy to see that there is a substantial difference in the way the metric distortion is distributed across the lobar patches. The two conformal methods CirclePack and LSCM tend to produce more inhomogeneous distribution of metric distortion, where the central regions of each lobar patch are contracted and the regions close to the boundary of the patch are expanded. This phenomenon is typical of conformal flattening methods for highly convoluted cerebral patches having relatively small boundaries.

Conclusions

LSCM preserved local angular information (shape) during flattening whereas CirclePack did not perform as well as expected due to the fact that the triangles of the cortical meshes were not equilateral. Adjustments to the default (tangency) circle packing approach such as non-tangency circle packings which preserve hyperbolic inversive distance (Bowers and Hurdal, 2003) may improve these results; inversive distance can be computed as a function of metric data from the triangle mesh. For all of the lobar patches, CirclePack ran extremely fast, which may be attributed to the increased number of boundary vertices. FreeSurfer outperformed both conformal methods with regard to the preservation of metric information I on the lobar patches and resulted in the most spatially homogeneous distribution of metric distortion; however, for the cerebral hemispheres, LSCM performed nearly as well as FreeSurfer and was clearly superior to FreeSurfer and CirclePack with regard to the preservation of angular information (shape information), metric information II, and computational efficiency. Whereas FreeSurfer required 631 min to produce a spherical surface map of the MNI hemisphere with angular and metric distortion of 18.75°, 26.06% (metric distortion I) and 18.88% (metric distortion II), respectively, LSCM required only 10 min to produce a similar map from the same mesh with angular and metric distortion of 4.63°, 33.70% and 11.79%; similar results were obtained for the UPENN hemisphere (Table 5). Compared to the other two algorithms, LSCM benefits from a more numerically robust optimization method.

Acknowledgments

This work is supported in part by NIH grant MH57180 and NSF grant DMS101339. Special thanks go to Dr. Bruce Fischl of Harvard University for assistance with FreeSurfer. The authors would also like to acknowledge Bill Wood from the Department of Mathematics at Florida State University for assistance with processing some of the data. The authors wish to thank the referees for their very helpful comments and suggestions.

References

Ahfors, L.V., 1996. Complex Analysis. McGraw-Hill Book Company, New York.

Angenent, S., Haker, S., Tannenbaum, A., Kikinis, R., 1999. Laplace–Beltrami operator and brain surface flattening. IEEE Trans. Med. Imag. 18, 700–711.

Brechbuhler, C., Gerig, G., Kubler, O., 1995. Parametrization of closed surfaces for 3-D shape description. Comput. Vis. Image Underst. 61, 154–170.

Bowers, P.L., Hurdal, M.K., 2003. Planar conformal mappings of piecewise flat surfaces. In: Hege, H.-C., Polthier, K. (Eds.), Visualization and Mathematics III. Springer Verlag, Berlin, pp. 3–34.

Collins, C., Stephenson, K., 2003. A circle packing algorithm. Comput. Geom.: Theory Appl. 25, 233–256.

Dijkstra, E.W., 1959. A note on two problems in connexion with graphs. Numer. Math. 1, 269–271.

Drury, H.A., Van Essen, D.C., Anderson, C.H., Lee, C.W., Coogan, T.A., Lewis, J.W., 1996. Computerized mappings of the Cerebral cortex: a multiresolution flattening method and a surface-based coordinate system. J. Cogn. Neurosci. 8, 1–28.

Fischl, B., Sereno, M.I., Dale, A.M., 1999. Cortical surface-based analysis II: inflation, flattening, and a surface-based coordinate system. NeuroImage 9, 179–194.

Gu, X.F., Yau, S.T., 2002. Computing conformal structures of surfaces. Commun. Inform. Syst. 2, 121–146.

Hurdal, M.K., Stephenson, K., 2004. Cortical cartography using the discrete conformal approach of circle packings. NeuroImage 23, s119–s128.

Hurdal, M.K., Bowers, P.L., Stephenson, K., Sumners, D.W.L., Rehm, K., Schaper, K., Rottenberg, D.A., 1999. Quasi-conformally flat mapping the human cerebellum. Lect. Notes Comput. Sci. 1679, 279–286.

Holmes, C.J., Hoge, R., 1996. Enhancement of T1 MR images using registration for signal averaging. The Journal of Neuroscience 3, S28.

Ju, L., Stern, J., Rehm, K., Schaper, K., Hurdal, M., Rottenberg, D., 2004. Cortical surface flattening using least squares conformal mapping with minimal metric distortion. Proceedings of ISBI'04, Arlington, VA, pp. 77–80.

Kanai, T., Suzuki, H., 2001. Approximate shortest path on a polyhedral surface and its applications. Comput. Aided Des. 33, 801–811.

Lorensen, W.E., Cline, H., 1987. Marching cubes: a high resolution 3D surface construction algorithm. Comput. Graph. 21, 163–169.

Levy, B., Petitjean, S., Ray, N., Malliot, J., 2002. Least squares conformal maps for automatic texture atlas generation. Proceedings of ACM SIGGRAPH'02. Addison Wesley.

Mitchell, J.S.B., Mount, D.M., Papadimitriou, C.H., 1987. The discrete geodesic problem. SIAM J. Sci. Comput. 16, 647–668.

Powell, M.J.D., 1964. An efficient method for finding the minimum of a

function of several variables without calculating derivatives. Comput. J. 7, 155–162.
Press, W.H., Teukolsky, S.A., Vetterling, W.T., Flannery, B.P., 1994. Numerical Recipe in C. Cambridge Univ. Press.
Rodin, B., Sullivan, D., 1987. The convergence of circle packings to the Riemann mapping. J. Differ. Geom. 26, 360–369.
Szekely, G., Kelemen, A., Brechbuehler, C., Gerig, G., 1996. Segmentation of 3D objects from MRI volume data using constrained elastic deformations of flexible Fourier surface models. Med. Image Anal. 1, 19–34.
Schmahmann, J.D., Doyon, J., Toga, A.W., Petrides, M., Evans, A.C., 2000. MRI Atlas of the Human Cerebellum. Academic Press, San Diego.
Schwartz, E.L., Merker, B., 1986. Computer-aided neuroanatomy: differential geometry of cortical surfaces and an optimal flattening algorithm. IEEE Comput. Graph. Appl. 6, 36–44.
Van Essen, D.C., Drury, H.A., Joshi, S., Miller, M.I., 1998. Functional and structural mapping of the human cerebral cortex: solutions are in the surfaces. Proc. Nat. Acad. Sci. 95, 788–795.